UNIVERSIDAD AUTÓNOMA DE NUEVO LEÓN
FACULTAD DE INGENIERÍA CIVIL

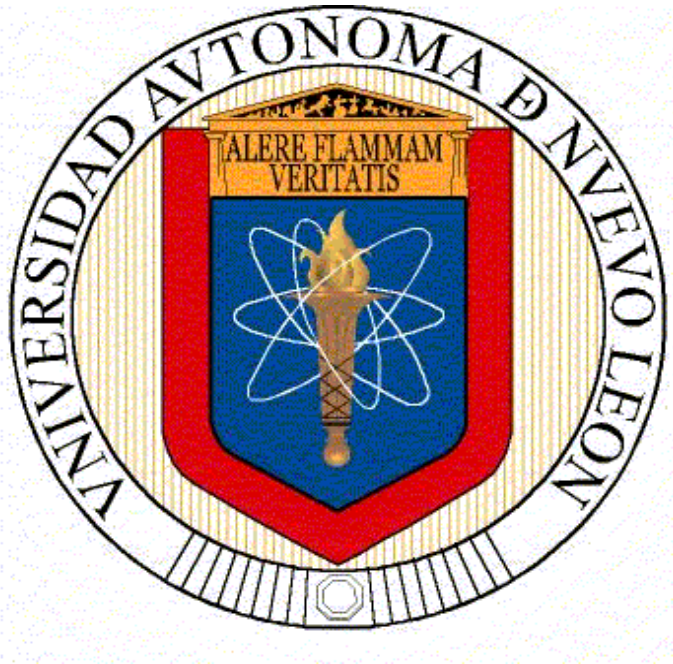

"A COMPOSITE DISCRETE TRACTION VECTOR"

QUE PRESENTA

GUILLERMO FERNANDO DÍAZ ORTIZ

PARA OBTENER EL GRADO DE
MAESTRÍA EN CIENCIAS CON ORIENTACIÓN EN INGENIERÍA ESTRUCTURAL

ABRIL 2013

UNIVERSIDAD AUTONOMA DE NUEVO LEÓN

TESIS MAESTRÍA

A COMPOSITE DISCRETE TRACTION VECTOR

Autor:
GUILLERMO FERNANDO DÍAZ ORTÍZ

Director de Tesis:
DR. JORGE HUMBERTO CHAVEZ

Abril 3, 2013

Part I

Preliminary

Acta

Esta tesis fue leida el día.....en la Universidad Autónoma de Nuevo Leon. Obteniendo la calificación de .....
.....

El Presidente

El Secretario

_____

_____

El Vocal

El Vocal

_____

_____

El Vocal

_____

Dedicatoria

A mis tres mosqueteras, Ana, Anita y Maria.
Tengo la familia mas bella que yo podía desear.

To my three musketeers, Ana, Anita y Maria.
I have the most beautiful family that I could wish for.

A mis padres, quien sin su soprte económico no hubiera sido posible estudiar mi maestría.
To my parents who without their economic support it would have been impossible to study my Master.
YAVEH-JHS-SS and MTAS, With all my love.

Contents

Glossary of notations

Greek letter

$\boldsymbol{\epsilon^c}$ composite material strain tensor, see equation (2.1), page (19) .

ϵ^f_{rr} f-th fiber extensional strain, see equation (2.1), page (19) .

$\boldsymbol{\epsilon^m}$ matrix strain tensor, see equation (2.1), page (19) .

γ^f_{rs} f-th fiber shear strains, see equation (2.1), page (19) .

γ^f_{rt} f-th fiber shear strains, see equation (2.1), page (19) .

ν^m matrix Poisson´s ratio, see equation (1.8), page (7) .

ρ^c_o mass of the composite, see equation (1.8), page (7) .

$\boldsymbol{\Sigma}(\boldsymbol{\epsilon}^c)$ constitutive function returning the composite stress in terms of the composite strains, see equation (1.8), page (7) .

Latin letter

$\boldsymbol{b}^c(\boldsymbol{x}, t)$ composite body forces vector, see equation (1.8), page (7) .

$\boldsymbol{r}^f$ f-th orthogonal reference system component, see equation (2.1), page (19) .

$\boldsymbol{s}^f$ f-th orthogonal reference system component, see equation (2.1), page (19) .

t^* prescribed traction vector, see equation (1.8), page (7) .

$\boldsymbol{t}^f$ f-th orthogonal reference system component, see equation (2.1), page (19) .

$\boldsymbol{u}$ displacements, see equation (1.8), page (7) .

$\boldsymbol{u}^*$ prescribed displacements, see equation (1.8), page (7) .

List of figures

List of boxes

Part II

Intoduction

1

Introduction

While many engineering problems can be treated in just two dimensions, some complex situations demand full three-dimensional analysis. Nowadays, with the advance in material research and the rapid progress in computer machines, three-dimensional analysis can be performed within affordable time and numerical cost. In this dissertation, a recent development in full three-dimensional analysis for reinforced concrete (RC) members is presented, which is an important step towards the development of versatile computational tools to model complex material behaviors.

The main concepts in constructing a three-dimensional RC tetrahedron are similar to the two-dimensions alone, which is idealized as a composite material consisting of plain concrete with reinforcement to be superimposed, by combining the constitutive laws expressed in terms of average stress and average strain of concrete and reinforcement. On the other hand, the numerical analysis of material failure, applied to RC members, represents an important tool for the safety estimation of engineered structures.

Despite of the considerable effort of more than four decades of research, in the numerical analysis of RC structural members, such as slabs, beams, columns and footings, they still present a challenge to the scientific community. These structural members are subjected to complex loading combinations. Section forces such as axial and bending moments induce longitudinal stresses, while shear forces and torsion moments induce shear as well as normal stresses due to diagonal cracking. The simultaneous action of both types of loading induces a complex stress-state, requiring the consideration of the interaction between normal and shear stresses. This complex interaction problem is the main topic of this dissertation.

The lack of reliability in predictions and the fact that the model parameters often have to be adapted to the structure, in order to obtain a good agreement with experimental data, has motivated the search for improved models of RC structural members.

Many questions are still unsatisfactorily answered and are been currently discussed inside the research community. The numerical modeling of the RC members probably started in the late 60s and early of the 70s, with the seminal works by Rashid [62], Ngo and Scordelis [55], Evans and Marathe [28] .

The complexity of RC analytical models, which arises when attempting to model a quasi-fragile material (plain concrete), and a ductile material (steel bars), leads to a combination of highly non-linear effects, as well as the description of failure processes in this cohesive-frictional material equipped with longitudinal steel bars at bending and steel stirrups at shear, which are characterized mainly by strain-softening phenomena (documented by Nádai 1931 in his seminal monograph of **plasticity** [53]), multiple cracking (in traction) and crushing (in compression), among others.

The constitutive equation of RC is an essential ingredient of any structural calculation. It provides the indispensable relation between strains and stresses, which is a linear relation in the case of elastic analysis and a much more complex nonlinear relation in nonlinear analysis, when the fracture processes comes into play, involving time and additional internal variables. In this dissertation we limit ourselves mainly to considering the "Continuum" mechanics approach, i.e., the Representative Volume Element (RVE) of material is considered as subject to a near-uniform macroscopic stress.

This Continuum assumption is equivalent to neglecting the local heterogeneity of the stresses and strains within the RVE, working with averaged quantities, as the effects of the heterogeneities, ignoring the effects of the aggregates (fragility or hardness),or the relationship between cement and water and aggregates. These materials require, constitutive laws with a decreasing stress under increasing strain, in the zone where inelastic processes appear. It is well known that, these structural members have a stable growth of multiple cracking, before the maximum pick-load is reached.

Unfortunately, because of this type of numerical response, it is a major task in science, not to mention the numerical treatment, to obtain the mechanical behavior ***post-pick-load***. Several constitutive models have been proposed in the literature for various RC behaviors, and with different levels of numerical sophistication.

Most of these phenomenological models treat concrete as a homogeneous single phase material (Damage theories, see e.g. Carol and William [7], Chaboche [8, 9], Chow and Wang [11], Cordebois and Sidoroff [15], Costin [16], Davidson and Stevens [17], Dougill [22], Dragon and Mróz [23], Han and Chen [34], Hueckel and Maier [35], Ju [37], Kachanov [38], Krajcinovic and Fonseka [39], Ladevéze [40], Lubarda et al. [42], Maier and Hueckel [43], Mazars and Lemaitre [45], Mazars and Pijaudier-Cabot [46], Ortiz [59], Simo and Ju [65, 66], Suaris and Shah [68], Yazdani and Schreyer [72]). Many questions are still unanswered, as regards reinforced concrete behavior. However, various publications on plain concrete, ***based on plasticity***, have been proposed in the last three decades, through different approaches, such as, the works by [Menétrey and William [49], Etse [27], Feenstra [29], Pramono and William [61], Menétrey et al. [48], Feenstra et al. [30], Grassl et al. [32]].

Unfortunately, the complex failure process in reinforced concrete, is characterized by stiffness degradation and irreversible deformation, whereby, a combination of stress-based scalar damage and plasticity, can be found in [Willam and Warnke [71], Meschke et al. [50], Bielger and Mehrabadi [6], Lee and Fenves [41], Grassl and Jirásek [31], Mohamad Hussein and Shao [52], Cicekli et al. [13], Chiarelli and Shao [10], Contrafatto and Cuomo [14], Červenka and Papanikolaou [69], Jason et al. [36]].

Several formulations also exist, based on micro-mechanics [Mattei et al. [44], Christoffersen et al. [12], Mehrabadi et al. [47], Nemat-Nasser and Mehrabadi [54], Oda et al. [56]]. The approach based on micro-planes, Bažant et al. [5, 2] , is very similar to the approach developed in the literature on micro-mechanics descriptions of granular materials, with the difference that they act only indirectly through a certain number of "internal variables". Moreover, in the framework of the "local state" assumption of Continuum Thermo-mechanics, it is considered that the state of a material point (and of its immediate vicinity in the sense of the RVE) is independent of that of the neighboring material point.

Therefore the stress strain gradient does not enter into the constitutive equation. These assumptions are obviously questioned in recent theories and congresses on "Continuum Mechanics", although these theories are not addressed here. Moreover, another formulation the so-called the “smeared approach” ((which treats the cracked material as an equivalent continuum) [Rice [63], Bažant and Oh [3], Červenka and Gerstle [70], DeBorst [18], Rots and Blaauwendraad [64]] can be found in the literature. Apparently [Barenblatt [1], Dugdale [24], Rashid [62]] were pioneer in the field of cohesive crack models.

Alternatively, Eringen [25, 26] and Bažant and Pijaudier-Cabot [4], Pijaudier-Cabot and Bažant [60] proposed a nonlocal plasticity and damage model respectively. In the 90‘s, various enhanced constitutive models, were proposed, among which, gradient-enhanced models stand out [DeBorst and Mühlhaus [21], Mühlhaus and Aifantis [51]], Cosserat continua [DeBorst [19], Steinmann and William [67]]. It is well known that, the numerical simulation of reinforced concrete behavior, many leads to some difficulties, due mainly to high ***strain localization***, which corresponds to multiple crack formation, this usually ocurrs when the maximum tensile or compressive strength of the plain concrete are exceeded in some material points of the structural member.

This phenomenon is commonly denoted as ***localization of deformation***, and has been documented by a wide range of authors, and is mainly the responsible for the loss of ellipticity, the lack of invariance with respect to the spatial discretization and the need for enhanced continuum models to overcome this problem.

The mathematical and numerical implications of this phenomenon can be found in DeBorst [20] , as well as an overview and references to this topic. We conclude this short introduction with the following idea, there are good reasons to believe that, in this century, the scientific community will find a good constitutive and computational modeling for reinforced concrete in order to overcome, the mixture of highly non-linear effects, such as, mathematical deficiency, i.e., the so called´´ill-posed proble´´; nonlinear effects in the interface between plain concrete and steel bars; multiple crushing in the structural members, multiple cracking in traction; nonlinear shear effects, and the correct instant of bifurcation, among others, and thus be able to find a responding complex structural members.

1.1 The fracture process in members of reinforced concrete

It is commonly accepted that the characterization to obtain the zone where the fracture process occur it is made through a specific transition between the materials that make up the continuum media. Typically, the contact surface between a quasi-brittle material like concrete a plastic material, like steel bars, make the

behavior of this zone highly nonlinear. On the one hand, we characterize the matrix in tensile stress regimes by a progressive softening, for which the stress decreases with increasing deformation

As shown in Oliver et al. [58] , the formation process of a strong discontinuity can be modeled as a weak discontinuity that collapses into a strong discontinuity at a certain time during the deformation process. However, the key question is: what happens when the steel bars form a cage, generating a confined core in the structural member? Because if the core is subjected to high compression states, the strong discontinuity generated by the states of tension cannot evolve. (**See Fig.(1.1)**).

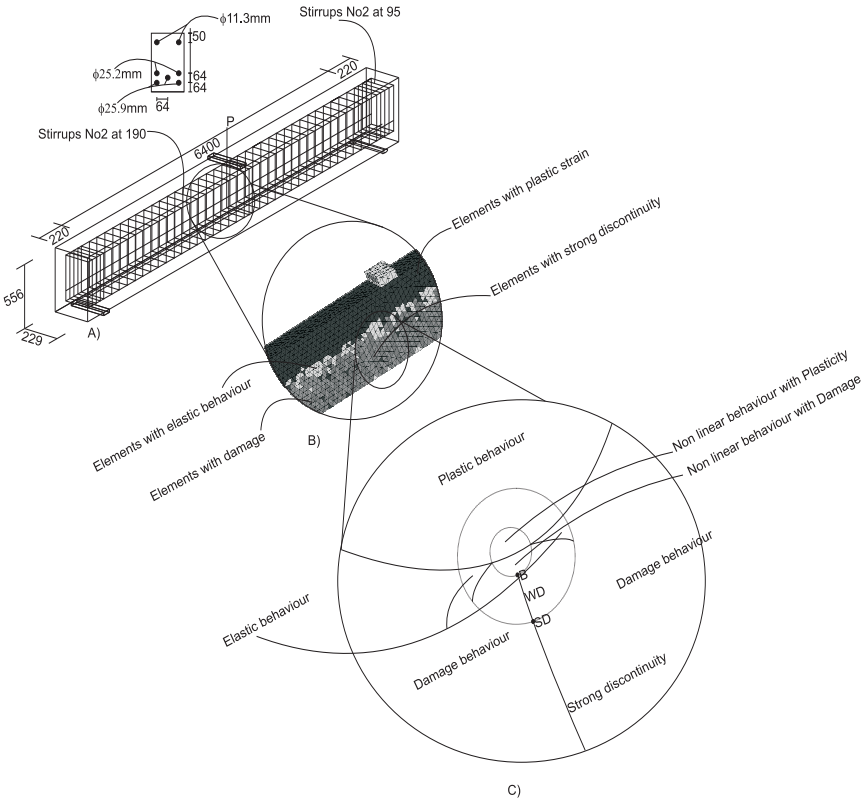

Figure 1.1: *Failure process of a structural member of reinforced concrete. a) Dimensions and geometry. b) Numeric representation and c) Schematic of the mechanical behavior in a failure state*

The motivation of this research is oriented towards obtaining a numerical composite model that is both robust and stable, and providing a numerical answer in failure states of a RC structural member subjected to high compression states. For this purpose, we use the classical equations of the quasi-static boundary value problem, but incorporating two extra equations of continuity, as shown in the following two sections.

1.1.1 Boundary value problem for composite material. Multi-field format

When localization of deformation, or "strain localization" in reinforced concrete, is modeled with a standard, inviscid reinforced concrete continuum model, a change occurs in character of the set of differential equations describing the motion and deformation of the continuum media. Attempts to capture the crack in reinforced concrete and other localization phenomena via numerical methods started in the 80s.
. The solution appeared to be linked to the fineness and the direction of the discretization of the mesh, However,

the main reason seemed to consist in the loss of ellipticity of the set of partial differential equations for the quasi-static case. In this case, the rate boundary value problem was ill-posed and numerical solutions suffered from spurious mesh sensitivity. To remedy this problem, one must either introduce additional terms in the set of differential equations governing the problem.
The main idea is then that the enhanced continuum model should reflect the micro-structural changes that occur when a material is stressed close to its failure limit. This prevents these equations from changing type during the loading process, and enables physically meaningful solutions to be obtained for the entire loading process. However, at least two out of four elements are needed to describe the kinematics of the localization zone properly, not to mention the fineness of the mesh required to capture the reinforcing bars. When attempting to model RC structural members, the required number of elements may become prohibitively large. With this argument in mind, we begin our work with the introduction of the basic notation, and briefly discuss the governing equations for a continuous body with discontinuity in a field of displacements.

1.1.2 Traction continuity

Let us also denote $\boldsymbol{\epsilon}^{\boldsymbol{c}}_{\Omega\setminus\mathbb{S}} = \boldsymbol{\epsilon}^{\boldsymbol{c}}|_{\boldsymbol{x}\in\Omega\setminus\mathbb{S}}$, $\boldsymbol{\sigma}^{\boldsymbol{c}}_{\Omega\setminus\mathbb{S}} = \boldsymbol{\sigma}^{\boldsymbol{c}}|_{\boldsymbol{x}\in\Omega\setminus\mathbb{S}}$ and $\boldsymbol{\epsilon}^{\boldsymbol{c}}_{\mathbb{S}} = \boldsymbol{\epsilon}^{\boldsymbol{c}}|_{\boldsymbol{x}\in\mathbb{S}}$, $\boldsymbol{\sigma}^{\boldsymbol{c}}_{\mathbb{S}} = \boldsymbol{\sigma}^{\boldsymbol{c}}|_{\boldsymbol{x}\in\mathbb{S}}$, as the composite strains and stresses at the continuous bulk of the body and in the discontinuous interface $\mathbb{S}$, respectively. The key point in the mechanics of fracture through the continuum mechanics is that we need to postulate the traction continuity across the discontinuity interface $\mathbb{S}$.The total and rate form of the traction vector can be stated the following manner:

$$\begin{aligned}
\boldsymbol{\sigma}^{\boldsymbol{c}}_{\Omega^+\setminus\mathbb{S}}.\boldsymbol{n} = \boldsymbol{\sigma}^{\boldsymbol{c}}_{\Omega^-\setminus\mathbb{S}}.\boldsymbol{n} = \boldsymbol{\sigma}^{\boldsymbol{c}}_{\mathbb{S}}.\boldsymbol{n} = \mathbb{T}(\boldsymbol{x},t) \quad \forall \boldsymbol{x}\in\mathbb{S}\wedge\forall t[0,\infty] \\
\dot{\boldsymbol{\sigma}}^{\boldsymbol{c}}_{\Omega^+\setminus\mathbb{S}}.\boldsymbol{n} = \dot{\boldsymbol{\sigma}}^{\boldsymbol{c}}_{\Omega^-\setminus\mathbb{S}}.\boldsymbol{n} = \dot{\boldsymbol{\sigma}}^{\boldsymbol{c}}_{\mathbb{S}}.\boldsymbol{n} = \dot{\mathbb{T}}(\boldsymbol{x},t) \quad \forall \boldsymbol{x}\in\mathbb{S}\wedge\forall t[0,\infty]
\end{aligned} \tag{1.1}$$

in which $\boldsymbol{\sigma}^{\boldsymbol{c}}_{\Omega^+\setminus\mathbb{S}} = \boldsymbol{\sigma}^{\boldsymbol{c}}_{\Omega\setminus\mathbb{S}}|_{\boldsymbol{x}\in\partial\Omega^+\cap\mathbb{S}}$ and $\boldsymbol{\sigma}^{\boldsymbol{c}}_{\Omega^-\setminus\mathbb{S}} = \boldsymbol{\sigma}^{\boldsymbol{c}}_{\Omega\setminus\mathbb{S}}|_{\boldsymbol{x}\in\partial\Omega^-\cap\mathbb{S}}$ are considered. In **Eq. (1.1)**, $\boldsymbol{\sigma}^{\boldsymbol{c}}_{\mathbb{S}}$ and $\dot{\boldsymbol{\sigma}}^{\boldsymbol{c}}_{\mathbb{S}}$ are the total and rate form of the composite stress at a given material point of the discontinuous interface $\mathbb{S}$ and $\boldsymbol{\sigma}^{\boldsymbol{c}}_{\Omega^+\setminus\mathbb{S}}$ and $\boldsymbol{\sigma}^{\boldsymbol{c}}_{\Omega^-\setminus\mathbb{S}}$ are the composite stresses at a neighbor point on the continuum part of the body $\Omega^+\setminus\mathbb{S}$ and $\Omega^-\setminus\mathbb{S}$, respectively. Before addressing crack models, we begin with a brief explanation of one of the most interesting phenomena that occurs in part of the plain and reinforced concrete members.

1.1.3 Composite governing equations

For the infinitesimal strain, rate=independent case, the problem can be stated as follows: consider a body formed by material points occupying a domain (Ω), with boundary $\partial\Omega = \Gamma_u \cup \Gamma_\sigma$ (where Γ_u is the part of the boundary with prescribed displacements and Γ_σ is the part of the boundary with prescribed tractions). The rate form of the governing equations describing the boundary value problem of composite material, in a time interval $[0,T]$, can be written as:

Box 1.1: *Quasistatic boundary value problem (BVP) for the composite material.*

Find:

$$\begin{cases} \dot{\boldsymbol{u}}(\boldsymbol{x},t) \\ \dot{\boldsymbol{\epsilon}}^c(\boldsymbol{x},t) \\ \dot{\boldsymbol{\sigma}}^c,(\boldsymbol{x},t) \end{cases}$$

Satisfying:

$\boldsymbol{\nabla}.\dot{\boldsymbol{\sigma}}^c + \rho_o^c \dot{\boldsymbol{b}}^c = 0$	$\forall(\boldsymbol{x},t) \in \Omega/\mathbb{S}$	Internal equilibrium	(1.2)
$\dot{\boldsymbol{\epsilon}}^c - \boldsymbol{\nabla}^s \dot{\boldsymbol{u}} = 0$	$\forall(\boldsymbol{x},t) \in \Omega \quad \times [0,T]$	Kinematical compatibility	(1.3)
$\dot{\boldsymbol{\sigma}}^c - \dot{\boldsymbol{\Sigma}}(\boldsymbol{\epsilon}^c) = 0$	$\forall(\boldsymbol{x},t) \in \Omega \quad \times [0,T]$	Constitutive compatibility	(1.4)
$\dot{\boldsymbol{\sigma}}^c.\boldsymbol{n} = \dot{t}^*$	$\forall(\boldsymbol{x},t) \in \Gamma_{\boldsymbol{\sigma}} \quad \times [0,T]$	External equilibrium	(1.5)
$\dot{\boldsymbol{u}} = \dot{\boldsymbol{u}}^*$	$\forall(\boldsymbol{x},t) \in \Gamma_{\boldsymbol{u}} \quad \times [0,T]$	Prescribed displacement	(1.6)
$\dot{\boldsymbol{\sigma}}^c_{\Omega^+}.\boldsymbol{n} - \dot{\boldsymbol{\sigma}}^c_{\Omega^-}.\boldsymbol{n} = 0$	$\forall(\boldsymbol{x},t) \in \mathbb{S} \quad \times [0,T]$	Outer traction continuity	(1.7)
$\dot{\boldsymbol{\sigma}}^c_{\Omega^+}.\boldsymbol{n} - \dot{\boldsymbol{\sigma}}^c_{\mathbb{S}}.\boldsymbol{n} = 0$	$\forall(\boldsymbol{x},t) \in \mathbb{S} \quad \times [0,T]$	Inner traction continuity	(1.8)

where ρ_o^c is the mass of the composite, $\boldsymbol{b}^c(\boldsymbol{x},t)$ is the composite body forces vector, t^* is the prescribed traction vector, $\boldsymbol{n}$ is the outward normal, $\boldsymbol{\Sigma}(\boldsymbol{\epsilon}^c)$ stands for the constitutive function returning the composite stress in terms of the composite strains $\boldsymbol{\epsilon}^c$, and finally, $\boldsymbol{u}$ and $\boldsymbol{u}^*$ are the displacements and prescribed displacements, respectively, as in **Fig.(1.2)**. [See **Remark 1.1**]

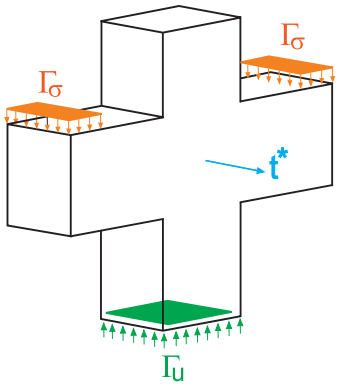

Figure 1.2: *Boundary value problem*

Remark 1.1 *After explicit imposition of* ***Eq. (1.4)*** *in to* ***Eqs.(1.2),(1.7)*** *and* ***(1.8)*** *, the typical two field (*$\boldsymbol{u}$ *and* $\boldsymbol{\epsilon}^c$*) problem can be rewritten. See Oliver et al. [57] .*

The **Eqs. (1.2)** to **(1.4)** represent the governing equations for composite materials (solids) without discontinuities. The outer traction continuity **Eq. (1.7)** may also be expressed as:

$$[\![\dot{\boldsymbol{\sigma}}^c_\Omega]\!] \equiv \dot{\boldsymbol{\sigma}}^c_{\Omega^+}.\boldsymbol{n} - \dot{\boldsymbol{\sigma}}^c_{\Omega^-}.\boldsymbol{n} = 0 \qquad \forall(\boldsymbol{x},t) \in \mathbb{S} \times [0,T] \tag{1.9}$$

From now on, the symbol $[\![\bullet]\!] := \bullet_+ - \bullet_-$ denotes the jump of an arbitrary quantity across $\mathbb{S}$.

Remark 1.2 *The function spaces for $\dot{\boldsymbol{u}}(\boldsymbol{x},t)$, $\dot{\boldsymbol{\epsilon}}^c(\boldsymbol{x},t)$ and $\dot{\boldsymbol{\sigma}}^c,(\boldsymbol{x},t)$ are assumed to be defined in such a way that the Dirichlet type boundary conditions are automatically fulfilled.*

1.2 Strain localization

One of the most important questions in fracture mechanics applied to reinforced concrete members is undoubtedly, when, how, and where does the inelastic process of the strains occur? And under what conditions can the inelastic strain increments localize in one or more narrow bands, separated from the remaining part of the body by the weak discontinuity surface?
The answer to this is far from straightforward. What we know is that we can simulate numerically the strain field through the displacement field by maintaining it continuous, and so obtain the strain field with a jump. Once again, this is not straightforward. However, this issue has been studied over the last 20 years, thanks to which mathematical foundation and researcherś experience have been improving steadily.
Some research groups around the world are currently developing formulations to capture the phenomenon of strain localization, and are obtaining satisfactory responses when trying to compare experimental vs. numerical results. The onset of the inelastic process of the strains may be accompanied by the formation of bands of intense straining; the current strains can be still continuous and the jump appears only in the strain rate.
Let us now determine the necessary conditions for the existence of such a solution. Typically, by using the classical localization analysis developed by Hadamard [33] , one material point $\boldsymbol{x}_s$ of the discontinuous surface Γs can be loss of strain continuity. For convenience, let us also consider that the surface splits the body into two sub-domains Ω^+ and Ω^- (*see* **Fig.(1.3)**).

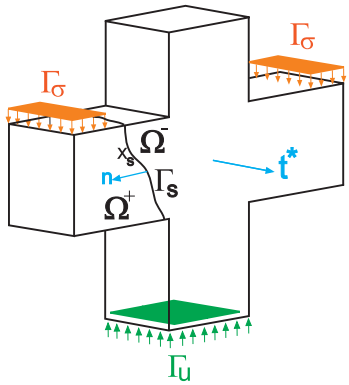

Figure 1.3: *Corbel of reinforced concrete split by a discontinuity surface*

According to Hadamard, if the point $\boldsymbol{x}_s$ is approached from Ω^+or from Ω^- (denoted by superscripts $+$ and $-$ on both sides of the discontinuity surface), certain fields that are discontinuous across Γ_s tend to different limits, for instance $\dot{\boldsymbol{\sigma}}^+$ and $\dot{\boldsymbol{\sigma}}^-$ denotes the stress rate on both sides of the discontinuity surface just next to point $\boldsymbol{x}_s$ respectively. Even though the stress and the strain rate can be discontinuous across a discontinuity surface, the corresponding jumps are not completely arbitrary. This is because the traction continuity condition constrained the stress rate jump. The same applies to the strain rate jump, which is limited by the displacement continuity condition. As defined in Hadamard [33] , the structure of the traction continuity condition can be written as follows:

$$\boldsymbol{n}\cdot\dot{\boldsymbol{\sigma}}^+ = \boldsymbol{n}\cdot\dot{\boldsymbol{\sigma}}^- \tag{1.10}$$

where $\boldsymbol{n}$ is the unit vector normal to Γ_s. In order to define the displacement continuity condition in terms of strain rates, let us define the continuous projection onto the cracks discontinuity surface, by employing a spatial gradient of a given displacement component, in the following manner:

$$\left[\frac{\partial \dot{\boldsymbol{u}}}{\partial \boldsymbol{x}}\right]^{+} = \left[\frac{\partial \dot{\boldsymbol{u}}}{\partial \boldsymbol{x}}\right]^{-} + \boldsymbol{r} \otimes \boldsymbol{n} \tag{1.11}$$

where $\boldsymbol{r}$ is an arbitrary vector and taking the form of $\boldsymbol{r} = \dot{\beta}\boldsymbol{m}$. The magnitude of the jump $\dot{\beta} = \|\boldsymbol{r}\|$ can be defined in terms of the unit first-order polarization tensor or normalized:

$$\boldsymbol{m} = \frac{\boldsymbol{r}}{\|\boldsymbol{r}\|} \tag{1.12}$$

implicitly holding the failure modes. By exploiting the symmetry of the strain tensor in the regime of small deformations, is straightforward to arrive at the displacement continuity condition in terms of strain rates as follows:

$$\boldsymbol{\epsilon}^{+} = \boldsymbol{\epsilon}^{-} + \dot{\boldsymbol{\beta}}(\boldsymbol{m} \otimes \boldsymbol{n})^{sym} \tag{1.13}$$

With all information given in this section, we can now begin to answer the questions posed at the beginning. To this end, we use the bifurcation analysis. First of all, we must obtain some expression that allows us to determinate the instant when the moment of fracture occurs. To this end, let us employ the following stain-stress equation:

$$\dot{\boldsymbol{\sigma}}^{+} = \mathbb{C}^{+}_{Tan}\dot{\boldsymbol{\epsilon}}^{+} \tag{1.14}$$
$$\dot{\boldsymbol{\sigma}}^{-} = \mathbb{C}^{-}_{Tan}\dot{\boldsymbol{\epsilon}}^{-} \tag{1.15}$$

In which $\mathbb{C}^{+}_{Tan}$ and $\mathbb{C}^{-}_{Tan}$ are the constitutive tangent operators on both sides of the discontinuity surface. Substituting the previous expressions into **Eqs.(1.10)** and **(1.13)** we obtain:

$$\boldsymbol{n} \cdot \mathbb{C}^{+}_{Tan} : \boldsymbol{\epsilon}^{-} + \left[\boldsymbol{n} \cdot \mathbb{C}^{+}_{Tan} : (\boldsymbol{m} \otimes \boldsymbol{n})^{sym}\right] \dot{\boldsymbol{\beta}} = \boldsymbol{n} \cdot \mathbb{C}^{-}_{Tan} : \boldsymbol{\epsilon}^{-} \tag{1.16}$$
$$\boldsymbol{n} \cdot \left[\mathbb{C}^{+}_{Tan} - \mathbb{C}^{-}_{Tan}\right] : \boldsymbol{\epsilon}^{-} = -\dot{\boldsymbol{\beta}} \left[\boldsymbol{n} \cdot \mathbb{C}^{+}_{Tan} \cdot \boldsymbol{n}\right] \cdot \boldsymbol{m} \tag{1.17}$$

thereby obtaining a general expression to describe a simple weak discontinuity. We analyzed the expression **Eq. (1.17)** . If the constitutive tangent operators are equal, the left hand side of this expression is zero, and a true discontinuity is obtained only with $\dot{\beta} \neq 0$. Then the previous equation we can be reduced as follows:

$$\underbrace{\left[\boldsymbol{n} \cdot \mathbb{C}^{+}_{Tan} \cdot \boldsymbol{n}\right]}_{\boldsymbol{Q}} \cdot \boldsymbol{m} = 0 \tag{1.18}$$

where the term in brackets is called the acoustic tensor. Since from a mathematical point of view, the singularity of this tensor (the acoustic or more precisely the localization tensor) indicates loss of ellipticity in quasi-static problems. Here the singularity of the localization tensor and the polarization unit first-order tensor $\boldsymbol{m}$, is its eigenvector associated with eigenvalue zero. The classical localization condition now takes the form:

$$det(\boldsymbol{Q}) = 0 \tag{1.19}$$

So, the key idea is to investigate when this condition ocurrs; by searching for a unit vector $\boldsymbol{n}$ for which the localization tensor becomes singular. The aim of the bifurcation analysis, is to find a unit vector $\boldsymbol{n}$for which the localization tensor becomes singular. It is noteworthy that, on the one hand if this vector $\boldsymbol{n}$ does not exist, the strains must remain continuous, and on the other hand, if we find a vector $\boldsymbol{n}$ that meets the condition of localization, this indicates that a strain jump can develop across a surface with normal $\boldsymbol{n}$. It is also important to mention that, if we explore **Eq. (1.18)** in deep, the acoustic tensor is a function of constitutive tangent operator. As we shall see later, this operator can be enriched in order to model material points of reinforced concrete.

1.3 Structure of the thesis

This work is structured into 4 chapters. An outline of the rest of the work is as follows: In *Chapter* 2 the fundamentals of strong discontinuity methodology applied to composite materials are given. The notions, of weak and strong kinematics, as well as a numerical technique of regularized kinematics of discontinuity applied to the composite material are given, but unlike of previous works by the author, the displacement field is enrich to capture multiples surfaces of strong discontinuities. The Obtain the composite discrete traction vector employee during this work, as well as the strong discontinuity conditions applied in the composite material are resolved in *Chapter* 3. *Chapter* 4 is devoted to a summary of the results obtained and to the concluding remarks. Possible extensions and improvements close out the thesis.

References

[1] Barenblatt, G. I. (1962). The mathematical thery of equilibrium of cracks in brittle fracture. *Adv. Appl. Mech.*, 7:55–129. 4

[2] Bažant, Z., Caner, F., Carol, I., Adley, M., and Akers, S. (2000). Microplane model m4 for concrete: I formulation with work -conjugate deviatoric stress. *Journal of Engineering Mechanics, ASCE*, 126(9):944–961. 4

[3] Bažant, Z. and Oh, B. (1983). Crack band theory for fracture of concrete. *Materials and Structures, RILEM*, 16(3):155–177. 4

[4] Bažant, Z. and Pijaudier-Cabot (1988). Nonlocal damage, localization, inestabilityand convergence. *Journal of applied mechanics*, 55:287–293. 4

[5] Bažant, Z., Xiang, Y., and Prat, P. (1996). Microplane model for concrete. i: Stress-strain boundaries and finite strain. *J. Struct. Eng, ASCE*, 122(3):245–254. 4

[6] Bielger, M. and Mehrabadi, M. (1995). An energy-based constitutive model for anisotropic solids subject to damage. *Mechanics of Materials*, 19(2-3):151–164. 4

[7] Carol, I. and William, K. (1996). Spurious energy dissipation/generation in modelling of stiffness recovery for elastic degradation and damage. *Internation journal of solids structure*, 33(20-22):2939–2957. 4

[8] Chaboche, J. (1990). *On the description of damage induced anisotropy and active-passive damage effects*, volume 109. Damage Mechanics in Engineering Materials, AMD, ASME. 4

[9] Chaboche, J. (1993). Development of continuum damage mechanics for elastic solids sustaining anisotropic and unilateral condition. *International journal Damage Mechanics*, 2(311-329). 4

[10] Chiarelli, A. and Shao, J. (2003). Modeling of elastoplastic damage behavior of a claystone. *International Journal of Plasticity*, 19(1):23–45. 4

[11] Chow, J. and Wang, J. (1987). An anisotropic theory of continuum damage mechanics for ductile fracture. *Engineering Fracture Mechanics*, 27(547-558). 4

[12] Christoffersen, J., Mehrabadi, M., and Nemat-Nasser, S. (1981). A micromechanical description of granular material behavior. *Journal of applied mechanics, ASME*, 48(2):239–344. 4

[13] Cicekli, U., Voyiadjis, G., and Abu Al Rub, R. (2007). A plasticity and anisotropic damage model for plain concrete. *International Journal of Plasticity*, 23(10-11):1874–1900. 4

[14] Contrafatto, L. and Cuomo, M. (2002). A new thermodynamically consistent continuum model for hardening plasticity coupled with damage. *International journal of solids and structures*, 39:6241–6271. 4

[15] Cordebois, J. and Sidoroff, F. (1982). Endommagement anisotrope en élasticité et plasticité. *J. de Mécanique Théorique et Appliquée*, pages 45–60. Numéro Spécial. 4

[16] Costin, L. (1985). Damage mechanics in post-failure regime. *Mech. Mater.*, 4(149-160). 4

[17] Davidson, L. and Stevens, A. (1973). Thermomechanical constitution of spalling elastic bodies. *J. Appl. Phys.*, 44:667–674. 4

[18] DeBorst, R. (1986). *Non-linear analysis of frictional materials*. PhD thesis, Delft University of Technology, The Netherlands. 4

[19] DeBorst, R. (1991). Simulation of strain localization: a reappraisal of the cosserat continuum. *Engineering Computations*, 8:317–332. 4

[20] DeBorst, R. (2001). Some recent issues in computational failure mechanics. *International Journal for Numerical Methods in Engineering*, 52:63–95. 4

[21] DeBorst, R. and Mühlhaus, H. (1992). Gradient dependant plasticity: formulation and algorithmic aspects. *International Journal for Numerical Methods in Engineering*, 3:521–539. 4

[22] Dougill, J. (1976). On stable progressively fracturing solids. *J. Appl. Math. Phys.*, 27:423–437. 4

[23] Dragon, A. and Mróz, Z. (1979). A continuum model for plastic-brittle behaviour of rock and concrete. *Int. J. Engng. Sci.*, 17:121–137. 4

[24] Dugdale, D. (1960). Yielding of sheets containing slits. *J. Mech. Phys. Solids*, pages 100–114. 4

[25] Eringen, A. (1981). On nonlocal plasticity. *International journal of Engineering Science*, 19:1461–1474. 4

[26] Eringen, A. (1983). Theories of nonlocal plasticity. *International journal of Engineering Science*, 21(741-751). 4

[27] Etse, G. (1992). *Theoretische und numerische untersuchung zum diffusen und lokalisierten versagen in beton*. PhD thesis, University of Karlsruhe. 4

[28] Evans, R. and Marathe, M. (1968). Microcracking and stress-strain curves for concrete in tension. *Materials and Structures*, 1(1):61–64. 3

[29] Feenstra, P. (1992). *Computational aspects of biaxial stress in plain and reinforced concrete*. PhD thesis, Delft University of Technology, The Netherlands. 4

[30] Feenstra, P., Rots, J., Amesen, A., Teigen, J., and Hoiseth, K. (1998). A 3d constitutive model for concrete based on co-rotational concept. *Proceedings of EURO-C*, 1:13–22. 4

[31] Grassl, P. and Jirásek, M. (2006). Damage-plastic model for concrete failure. *International journal of solids and structures*, 43:7166–7196. 4

[32] Grassl, P., Lundgren, K., and Gylltoft, K. (2002). Concrete in compression: a plasticity theory with a novel hardening law. *International Journal of Solids and Structures*, 20(5205-5223). 4

[33] Hadamard, J. (1903). Lecons sur la propagation des ondes et les equations de l´hydrodynamique. *Paris, Hermann*. 8

[34] Han, D. and Chen, W. (1986). Strain-space plasticity formulation for hardening-softening materials with elasto-plastic coupling. *International Journal of Solids and Structures*, 22:935–950. 4

[35] Hueckel, T. and Maier, G. (1977). Incrementally boundary value problem in the presence of coupling of elastic and plastic deformations: a rock mechanics oriented theory. *Internation journal of solids structure*, 13:1–15. 4

[36] Jason, L., Huerta, A., Pijaudier Cabot, G., and Ghavamian, S. (2006). An elastic-plastic damage formulation for concrete: aplication to elementary test and comparison with isotropic damage model. *Computer Methods in Applied Mechanics and Engineering*, 195(52):7007–7092. 4

[37] Ju, J. (1990). Isotropic and anisotropic damage variables in continuum damage mechanics. *ASCE, J. Engng. Mech.*, 116(12):2764–2770. 4

[38] Kachanov, L. (1958). Time of the ruptureprocess under creep conditions. *IVZ Akad. Nauk, S.S.R., Otd Tech Nauk*, 8:26–31. 4

[39] Krajcinovic, D. and Fonseka, G. (1981). The continuos damage theory of brittle materials. *J. Appl. Mech.*, 48:809–824. 4

[40] Ladevéze, P. (1983). Sur une theorie de lèndommagement anisotrope. Technical report, Laboratorie de Mechanique et Technologie, Escole Normale Superieure., 61, av. du Pdt. Wilson, 94235, Cachan Cedex, France. 4

[41] Lee, J. and Fenves, G. (1998). Plastic-damage model for cyclic loading of concrete structures. *Journal of Engineering Mechanics, ASCE*, 124(8):892–900. 4

[42] Lubarda, V., Krajcinovic, D., and Mastilovic, S. (1994). Damage model for brittle elastic solids with unequal tensile and compressive strengths. *Engng. Fract. Mech.*, 49(5):681–697. 4

[43] Maier, G. and Hueckel, T. (1979). Nonassociated and oupled flow rules of elastoplasticity for rock-like materials. *Int. J. Rock. Mech. Min. Sci. Geomech.*, 16:77–92. 4

[44] Mattei, N. J., Mehrabadi, M. M., and Zhu, H. (2007). A micromechanical constitutive model for the behavior concrete. *Mechanics of Materials*, 39:357–379. 4

[45] Mazars, J. and Lemaitre, J. (1984). Application of continuos damage mechanics to strain and fracture behavior of concrete. *Application of fracture mechanics to cementitous composites, NATO Advanced research worksop*, Northwestern university (Edited by S. P. Shah):375–388. 4

[46] Mazars, J. and Pijaudier-Cabot, G. (1989). Continuum damage theory -application to concrete. *ASCE, J. Engng. Mech.*, 115:345–365. 4

[47] Mehrabadi, M., Nemat-Nasser, S., and Oda, M. (1982). On statistical description of stress and fabric in granular materials. *Int. J. Num. Anal. Meth. Geomech.*, 6(95-108). 4

[48] Menétrey, P., Walther, R., Zimmermann, T., Willam, K., and Regan, P. (1997). Simulation of punching failure in reinforced-concrete structures. *Journal of Structural Engineering, ASCE*, 123(5):652–659. 4

[49] Menétrey, P. and William, K. (1995). Triaxial failure criterion for concrete and its generalization. *ACI Structural Journal*, 3:311–318. 4

[50] Meschke, G., Lackner, R., and Mang, H. (1988). An anisotropic elastoplastic-damage model for plain concrete. *International Journal for Numerical Methods in Engineering*, 42(4):703–727. 4

[51] Mühlhaus, H. and Aifantis, E. (1991). A variational principle for gradient plasticity. *International Journal of Solids and Structures*, 28:845–857. 4

[52] Mohamad Hussein, A. and Shao, J. (2007). Modelling of elastoplastic behaviour with non-local damage in concrete under compression. *Computers and Structures*, 85(23-24):1757–1768. 4

[53] Nádai, A. (1931). *Plasticity*. McGraw-Hill. 3

[54] Nemat-Nasser, S. and Mehrabadi, M. (1984). *Mechanics of Engineering Materials*. Desai, C.S. and Gallagher, R.H. John Wiley and Sons, New York, NY. 4

[55] Ngo, N. and Scordelis, A. (1967). Finite element analysis of reinforced concrete beams. *J. Am. Concr. Inst.*, 64:152–163. 3

[56] Oda, M., Nemat-Nasser, S., and Mehrabadi, M. (1982). A statistical study of fabric in a random assembly of spherical granules. *Int. J. Num. Anal. Meth. Geomech*, 6:77–94. 4

[57] Oliver, J., Huespe, A., and Samaniego, E. (2003). A study on finite elements for capturing strong discontinuities. *International journal for numerical methods in engineering*, 56:2135–2161. 7

[58] Oliver, J., Linero, D., Huespe, A., and Manzoli, O. (2008). Two-dimensional modeling of mterial failure in reinforced concrete by means of a continuum strong discontinuity approach. *Appl. Mech. Eng.*, 197(332-348). 5

[59] Ortiz, M. (1985). A constitutive theory for the inelastic behavior concrete. *Mech. Mater.*, (4):67–93. 4

[60] Pijaudier-Cabot, G. and Bažant, Z. (1987). Nonlocal damage theory. *Journal of Engineering Mechanics, ASCE*, 113:1512–1533. 4

[61] Pramono, E. and William, K. (1989). Fracture energy-based plasticity formulation of plain concrete. *Journal of Engineering Mechanics, ASCE*, 115:1183–1203. 4

[62] Rashid, Y. (1968). Analysis of prestressed concrete pressure vessels. *Nuclear Engineering and Design*, 7(4):334–344. 3, 4

[63] Rice, J. (1968). *Mathematical analysis in the mechanics of fracture*. Fracture , Academic Press. 4

[64] Rots, J. and Blaauwendraad, J. (1989). Crack models for concrete: discrete or smeared? fixed, multidirectional or rotating?. *Heron*, 34(1). 4

[65] Simo, J. and Ju, J. (1987a). Strain- and stress-based continuum damage models- i. formulation. *International journal of solids and structures*, 23(7):821–840. 4

[66] Simo, J. and Ju, J. (1987b). Strain- and stress-based continuum damage models- ii. computational aspects. *International journal of solids and structures*, 23(7):841–869. 4

[67] Steinmann, P. and William, K. (1991). *Localization within the framework of microplolar elasto-plasticity*. Advances in Continuum Mechanics. V. Mannl, and Najar, J. and Brüller, O. 4

[68] Suaris, W. and Shah, S. (1984). Rate-sensitivity damage theory for brittle solids. *ASCE, J. Engng. Mech.*, 110(6):985–997. 4

[69] Červenka, J. and Papanikolaou, V. K. (2008). Three dimensional combined fracture-plastic material model for concrete. *International journal of plasticity*, 24(12):2192–2220. 4

[70] Červenka, V. and Gerstle, K. (1971). Inelastic analysis of reinforced concrete panels part i: Theory. *Publication I.A.B.S.E.*, 31(11):32–45. 4

[71] Willam, K. and Warnke, K. (1974). Constitutive model for triaxial behaviour of concrete. *Proc. Concrete Struct. Subjected to triaxial stresses, Inst. Assoc. for Bridges and Struct. Eng.*, 19(3):1–30. 4

[72] Yazdani, S. and Schreyer, H. (1988). An anisotropic damage model with dilatation for concrete. *Mech. Mater.*, 7:231–244. 4

Part III

Three-dimensional formulation for reinforced concrete

Contents

2

Strong discontinuities applied to composite materials

THE main goal of the present chapter is the introduction of the kinematic of the multiple surface discontinuity, for project the dissipative composite constitutive model, equipped with strain softening, (on the part of the matrix), into a discrete traction-separation law, to fulfill the condition of the strong discontinuity applied in the composite materials.

2.1 A concise review of the fundamentals applied to the composite material

The aim of strong discontinuity analysis applied to composite materials is to identify those conditions that make the constitutive models using in previous works, make compatible with the strong discontinuity kinematic Mosler [9] . So, in order to fulfill these conditions, the remainder of this section is structured as follows: the original strong discontinuity kinematics applied to composite materials, as well as a weak kinematics are introduced in *Section(2.1.2)* . The reader interest in know how change from the weak to strong discontinuities, please see Oliver et al. [12] . Before describing the kinematics, let us define the composite strains through a simple assumption, using the mixture theory Atkin and Craine [2], Bowen [3], Eringen and Ingram [4], Ingram and Eringen [7], Green and Naghdi [6], Truesdell and Noll [19], Truesdell and Toupin [20] as follows:

2.1.1 Basic assumption for the composite material

It is assumed that all components share the same strains in **Fig.(2.1)** (compatibility concept or closing equation), that is:

$$\begin{aligned}
\boldsymbol{\epsilon}^{\mathbf{m}} &= \alpha\boldsymbol{\epsilon}^{\mathbf{c}} \\
\epsilon^{f}_{rr} &= (\eta)\boldsymbol{r}^{f}.\boldsymbol{\epsilon}^{\mathbf{c}}.\boldsymbol{r}^{f} \\
\gamma^{f}_{rs} &= (\eta)2\boldsymbol{r}^{f}.\boldsymbol{\epsilon}^{\mathbf{c}}.\boldsymbol{s}^{f} \\
\gamma^{f}_{rt} &= (\eta)2\boldsymbol{r}^{f}.\boldsymbol{\epsilon}^{\mathbf{c}}.\boldsymbol{t}^{f}
\end{aligned} \tag{2.1}$$

In **Eq. (2.1)**, $\boldsymbol{\epsilon}^{m}$ and $\boldsymbol{\epsilon}^{c}$ are the matrix and composite material strain tensor, respectively. This assumption is valid in the absence of atomic diffusion. The extensional strain of the f-th fiber ϵ^{f}_{rr}, in direction $\boldsymbol{r}^{f}$ is equal to the component of the composite strain field in that direction. In a local orthogonal reference system $\left(\boldsymbol{r}^{f}, \boldsymbol{s}^{f}, \boldsymbol{t}^{f}\right)$, the shear strains of the f-th fiber γ^{f}_{rs} and γ^{f}_{rt} are obtained as the shear components of the composite strain field, finally α and η are the parameters to try to discriminate the deformation that corresponds to each component.

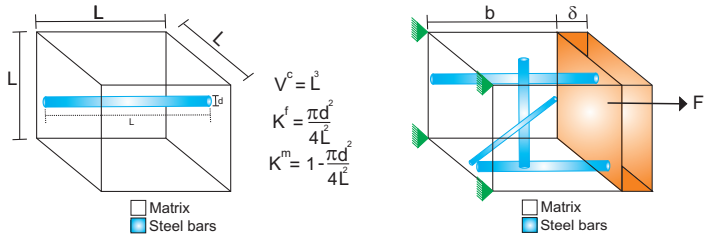

(a) *Volumetric fractions* **(b)** *Shared strain*

Figure 2.1: *Composite material*

2.1.2 Kinematics induced through strong discontinuities in composites materials

This section is concerned with the kinematics used in the composite material. Let us begin by establishing the kinematical relations for the non-linear composite model and their appropriate composite strain. We start by defining the fundamentals, accompanied by weak and strong discontinuities in order to establish the regularized kinematics of discontinuity in composite materials. It is important to define the kinematics of this mode (regularized kinematics), since allow introduce in a natural manner into the composite constitutive model.

2.1.2.1 Fundamentals

This section, consists of a short review of the fundamentals of the kinematics induced by strong discontinuities: for further details, refer to Simo et al. [18], Garikipati [5], Oliver [10, 11], Manzoli [8], Oliver et al. [12], Armero [1], Oliver et al. [15, 16, 17], Oliver and Huespe [14, 13] .

Let us consider a three-dimensional body $\Omega \subset \mathbb{R}^3$ [§] (more precisely, an open bounded set) assumed to be separated into two parts (Ω^+ and Ω^- through a $\Gamma_{\mathbb{S}}$) whose material points are labeled as $\boldsymbol{x}$, and a material (fixed along time) surface $\mathbb{S}$ [†] in Ω. Let us also consider an orthogonal system of curvilinear coordinates ξ, η and χ, such that $\mathbb{S}$ corresponds to the coordinate surface

$$\mathbb{S} := \{\boldsymbol{x}(\xi,\eta,\chi) \in \Omega \quad | \quad \chi = 0\} \tag{2.2}$$

In turn we can obtain the orthonormal base associated to that system of coordinates by $(\hat{e}_\xi, \hat{e}_\eta, \hat{e}_\chi)$, and finally we define the corresponding scale factors $\boldsymbol{r}_\xi(\xi,\eta,\chi)$, $\boldsymbol{r}_\eta(\xi,\eta,\chi)$ and $\boldsymbol{r}_\chi(\xi,\eta,\chi)$ such that:

$$\begin{aligned} d\mathbb{S}_\xi &= r_\xi d\xi \\ d\mathbb{S}_\eta &= r_\eta d\eta \\ d\mathbb{S}_\chi &= r_\chi d\chi \end{aligned} \tag{2.3}$$

are the differential arc lengths along the coordinates surface ξ, η respectively. We also follow the guidelines of the work by Manzoli [8] (See also Oliver et al. [12] , **Fig.(2.2)** and **Remark 2.1**). Here we extend the definition of bandwidth from $2D$ to $3D$ in **Eq. (2.5)**:

$$h(\xi,\eta) = r_\chi(\xi,\eta,\chi)(\chi^+ - \chi^-) \tag{2.4}$$

[§] The configuration occupied by a solid reference placement in $\Omega_0 \subset \mathbb{R}^3$ is denoted by $\boldsymbol{X}$.

[†] which from now on will be called discontinuity surface.

Remark 2.1 *Let us consider the surfaces $\mathbb{S}^+_\chi$ and $\mathbb{S}^-_\chi$, which coincide with the coordinates $\chi = \chi^+$ and $\chi = \chi^-$, enclosing a discontinuity band*

$$\Omega^h := \{\boldsymbol{x}(\xi,\eta,\chi) \quad | \quad \chi \in (\chi^+,\chi^-)\} \tag{2.5}$$

The introduction of these bandwidths induces a partition

$$\Omega = \Omega^+ \cup \Omega^- \cup \Gamma_u \cup \Gamma_\sigma \cap \Omega^h \tag{2.6}$$

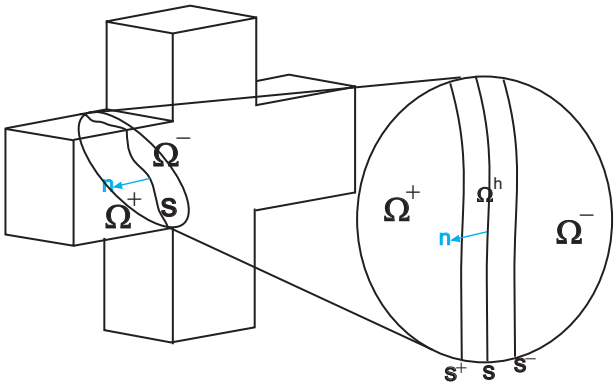

Figure 2.2: *Bandwith of strain localization*

2.1.2.2 Kinematics of weak discontinuities

The kinematics of a body Ω **Fig.(2.2)** containing a discontinuity (jump) of value $[\![\dot{\boldsymbol{u}}]\!](\boldsymbol{x},t)$ in the rate of the displacement field can be described in **Eq. (2.7)**.

$$\dot{\boldsymbol{u}}(\boldsymbol{x},t) = \dot{\tilde{\boldsymbol{u}}}(\boldsymbol{x},t) + \sum_{\beta=1}^{N_s} H^\beta_{\Omega^h}(\boldsymbol{x},t)[\![\dot{\boldsymbol{u}}]\!]^\beta(\boldsymbol{x},t) \tag{2.7}$$

where $\dot{\tilde{\boldsymbol{u}}}(\boldsymbol{x},t)$ and $[\![\dot{\boldsymbol{u}}]\!](\boldsymbol{x},t)$, are the regular resulting velocity and the velocity jump respectively, β is the surface of failure in study, N_s is the active localization surface(being the great difference with previous works). H_{Ω^h} is the unit ramp function and is a continuous function in Ω defined by:

$$H^\beta_{\Omega^h} := \begin{cases} 0 & \boldsymbol{x} \in \Omega^- \quad \chi \le \chi^- \\ 1 & \boldsymbol{x} \in \Omega^+ \quad \chi \ge \chi^+ \\ \dfrac{\chi - \chi^-}{\chi^+ - \chi^-} & \boldsymbol{x} \in \Omega^h \quad \chi^- < \chi < \chi^+ \end{cases} \tag{2.8}$$

In the **Eq. (2.8)** $H^\beta_{\Omega^h}$ contains a unit jump, different from its values at $\mathbb{S}^+$ and $\mathbb{S}^-$ for the same coordinate surface $\xi and \eta$:

$$\chi\,[\![H^\beta_{\Omega^h}]\!] = H^\beta_{\Omega^h}(\xi,\eta,\chi^+) - H^\beta_{\Omega^h}(\xi,\eta,\chi^-) = 1 \quad \forall\xi \wedge \forall\eta \tag{2.9}$$

The gradient of $H^\beta_{\Omega^h}$ is given in orthogonal curvilinear coordinates by:

$$\begin{aligned}\nabla H^{\beta}_{\Omega^h} &= \frac{\partial H^{\beta}}{\partial \xi}\frac{\partial \xi}{\partial \mathbb{S}_{\xi}}\frac{\partial \mathbb{S}_{\xi}}{\partial \boldsymbol{x}} + \frac{\partial H^{\beta}}{\partial \eta}\frac{\partial \eta}{\partial \mathbb{S}_{\eta}}\frac{\partial \mathbb{S}_{\eta}}{\partial \boldsymbol{x}} + \frac{\partial H^{\beta}}{\partial \chi}\frac{\partial \chi}{\partial \mathbb{S}_{\chi}}\frac{\partial \mathbb{S}_{\chi}}{\partial \boldsymbol{x}} \\ &= \frac{1}{r_{\xi}}\frac{\partial H^{\beta}_{\Omega^h}}{\partial \xi}\hat{e}_{\xi} + \frac{1}{r_{\eta}}\frac{\partial H^{\beta}_{\Omega^h}}{\partial \eta}\hat{e}_{\eta} + \frac{1}{r_{\chi}}\frac{\partial H^{\beta}_{\Omega^h}}{\partial \chi}\hat{e}_{\chi} \\ &= \mu_{\Omega^{h\beta}}\frac{1}{h_{\chi}}\hat{e}^{\beta}_{\chi}\end{aligned} \tag{2.10}$$

where μ_{Ω^h} is a collocation function, defined as:

$$\mu_{\Omega^{h\beta}} := \begin{cases} 0 & \boldsymbol{x} \notin \Omega^h \\ 1 & \boldsymbol{x} \in \Omega^h \end{cases} \tag{2.11}$$

Finally, we can obtain the kinematic compatible with the rate of strains of the composite $\boldsymbol{\epsilon}^c$ as follows:

$$\begin{aligned}\dot{\boldsymbol{\epsilon}}^c = \nabla^s \dot{\boldsymbol{u}} &= \nabla^s \dot{\bar{\boldsymbol{u}}} + \sum_{\beta=1}^{N_s} H^{\beta}_{\Omega^h} \nabla^s [\![\dot{\boldsymbol{u}}]\!](\boldsymbol{x},t) + \sum_{\beta=1}^{N_s} [\![\dot{\boldsymbol{u}}]\!](\boldsymbol{x},t) \nabla^s H^{\beta}_{\Omega^h} \\ &= \underbrace{\nabla^s \dot{\bar{\boldsymbol{u}}} + \sum_{\beta=1}^{N_s} H^{\beta}_{\Omega^h} \nabla^s [\![\dot{\boldsymbol{u}}]\!](\boldsymbol{x},t)}_{\dot{\bar{\boldsymbol{\epsilon}}}^c \quad \text{regular} \quad \forall(\boldsymbol{x})\in\Omega/\mathbb{S}} + \underbrace{\sum_{\beta=1}^{N_s} \mu_{\Omega^h} \frac{1}{h_{\chi}} ([\![\dot{\boldsymbol{u}}]\!](\boldsymbol{x},t) \otimes \hat{\boldsymbol{e}}_{\chi})^s}_{[\![\dot{\boldsymbol{\epsilon}}^c]\!] \quad \text{discontinuos} \quad \forall(\boldsymbol{x})\in\mathbb{S}}\end{aligned} \tag{2.12}$$

Remark 2.2 *The structure of the composite strain tensor* ***Eq. (2.12)*** *can be expressed as the sum of a term including only regular part* $\dot{\bar{\boldsymbol{\epsilon}}}^c$ *and a term which includes a singular part* $[\![\dot{\boldsymbol{\epsilon}}^c]\!]$.

References

[1] Armero, F. (1999). Large-scale modeling of localized dissipative mechanisms in a local continuum: applications to the numerical simulation of strain localization in rate-dependent inelastic solids. *Mech. Cohesive-Frictional Mater*, pages 101–131. 20

[2] Atkin, R. and Craine, R. (1976). Continuum theories of mixture basic theory and historical develpment. *Quant. J. Mech. Appl. Math.*, 29:209–244. 19

[3] Bowen, R. (1976). *Theory of mixture*. Academic Press, New York. A.C. Eringen, ed. Continuum Physic 3. 19

[4] Eringen, A. and Ingram, J. (1965). A continuum theory of chemically reacting media-i. *International journal of Engineering Science*, 3:197–212. 19

[5] Garikipati, K. (1996). *On strong discontinuities in inelastic solids and their numeriacal simulation*. PhD thesis, Standford University. 20

[6] Green, A. and Naghdi, P. (1965). A dynamic theory of interacting continua. *Int. J. Engng. Sci.*, 3:231–241. 19

[7] Ingram, J. and Eringen, A. (1967). A continuum theory of chemically reacting media-ii: Constitutive equations of reacting fluid mixtures. *Int. J. Engng. Sci.*, pages 289–322. 19

[8] Manzoli, O. (1998). *Un modelo analítico y numérico para la simulación de discontinuidades fuertes en la mecánica de sólidos*. PhD thesis, Universidad Politécnica de Cataluña. 20

[9] Mosler, J. (2005). Numerical analyses of discontinuous material bifurcation: strong and weak discontinuities. *Computer Methods in Applied Mechanics and Engineering*, 194:979–1000. 19

[10] Oliver, J. (1996a). Modelling strong discontinuities in solid mechanics via strain softening constitutive equations. part 1: Fundamentals. *International journal for numerical methods in engineering*, 39:3575–3600. 20

[11] Oliver, J. (1996b). Modelling strong discontinuities in solid mechanics via strain softening constitutive equations. part 2: Numerical simulation. *International journal for numerical methods in engineering*, 39:3601–3623. 20

[12] Oliver, J., Cervera, M., and Manzoli, O. (1999). Strong discontinuities and continuum plasticity models: the strong discontinuity approach. *Internation journal of plasticity*, 15(319-351). 19, 20

[13] Oliver, J. and Huespe, A. (2004a). Continuum approach to material failure in strong discontinuity settings. *Computer methods in applied mechanics and engineering*, 193:3195–3220. 20

[14] Oliver, J. and Huespe, A. (2004b). Theorical and computational issues in modelling material failure in strong discontinuity scenarios. *Computer methods in applied mechanics and engineering*, 193:2987–3014. 20

[15] Oliver, J., Huespe, A., and Samaniego, E. (2003a). A study on finite elements for capturing strong discontinuities. *International journal for numerical methods in engineering*, 56:2135–2161. 20

[16] Oliver, J., Huespe, A., Samaniego, E., and Chaves, E. (2003b). On the strong discontinuity approach in finite deformation settings. *International journal for numerical methods in engineering*, 56:1051–1082. 20

[17] Oliver, J., Huespe, A., Samaniego, E., and Chaves, E. (2004). Continuum approach to the numerical simulation of material failure concrete. *International journal for numerical and analytical methods in geomechanics*, 28:609–632. 20

[18] Simo, J., Oliver, J., and Armero, F. (1993). An analysis of strong discontinuities induced by strain-softening in rate-independent inelastic solids. *Computational mechanics*, 12(5):277–296. 20

[19] Truesdell, C. and Noll, W. (1965). *The non-linera field theories of mechanics*. Springer, Berlin, second edition. 19

[20] Truesdell, C. and Toupin, R. (1960). *The classical field theories*. First edition. 19

3

Composite discrete constitutive equation

The aim of this chapter is compute a composite discrete constitutive equation. For this purpose it is necessary use the composite discrete traction vector *Section(3.1)*, as well as the discrete free energy *Section(3.2)* and the strong discontinuity conditions for the composite material *Section(3.3)*.

3.1 Composite discrete constitutive equation

We start this section by considering a given point of the interface $\mathbb{S}$, at which each point is made up by a (plain concrete) matrix and steel bars (fibers). The key point is to consider various phenomena that occur at each material point, when the matrix moves in one step to tensile stress states, and in another step to compressive stress states, due to multiple-cracks formation mechanisms. These phenomena are complex and highly non-linear unfortunately. To model numerically the reinforced concrete, we need to incorporate the three effects of each fiber that made up the composite material. However unlike previous works, the composite discrete traction vector, will have information with multiple surface of failure activate.Thus the composite stresses and the composite strains given by the kinematics can incorporate as follows:

$$\boldsymbol{\sigma}^{c} = k^{m}\frac{q_{\mathbb{S}}}{r_{\mathbb{S}}}\mathbb{C}^{e^{m}} : \left[(\bar{\boldsymbol{\epsilon}} + \frac{1}{h}(\sum_{\beta=1}^{N_s}\Delta[\![\boldsymbol{u}^{\beta}]\!](\boldsymbol{x},t))\otimes\boldsymbol{n}^{\boldsymbol{\beta}})^{s} - \Delta\lambda^{p^{m}}\frac{\partial g^{p^{m}}}{\partial\boldsymbol{\sigma}^{\boldsymbol{m}}}\right] + \sum_{f=1}^{nf} k^{f}\left[E^{f}_{rr}\left(\epsilon^{f}_{rr} - \Delta\lambda^{p^{f}}\frac{\partial f^{p^{f}}_{rr}}{\partial {\sigma^{f}}_{rr}}\right)[\boldsymbol{r}^{f}\otimes\boldsymbol{r}^{f}] + \right.$$
$$\left. 2G^{f}_{rs}\left(\epsilon^{f}_{rs} - \Delta\lambda^{p^{f}}\frac{\partial f^{p^{f}}_{rs}}{\partial {\sigma^{f}}_{rs}}\right)[\boldsymbol{r}^{f}\otimes\boldsymbol{s}^{f}]^{s} + 2G^{f}_{rt}\left(\epsilon^{f}_{rt} - \Delta\lambda^{p^{f}}\frac{\partial f^{p^{f}}_{rt}}{\partial {\sigma^{f}}_{rt}}\right)[\boldsymbol{r}^{f}\otimes\boldsymbol{t}^{f}]^{s}\right] \tag{3.1}$$

So, we now consider for $t > t_{SD}$ the strong discontinuity regime for the composite material, i.e., when $h \equiv k \to 0$. Multiply the above equation by the normal vector we arrive at:

$$\mathbb{T}^{c^{\beta}}_{\mathbb{S}} = \boldsymbol{\sigma}^{c^{\beta}}_{\mathbb{S}}.\boldsymbol{n}^{\boldsymbol{\beta}} = \lim_{h\to 0} k^{m}\frac{q_{\mathbb{S}}}{r_{\mathbb{S}}}\boldsymbol{n}^{\boldsymbol{\beta}}.\mathbb{C}^{e^{m}} : \left[\bar{\boldsymbol{\epsilon}} + \frac{1}{h}(\Delta[\![\boldsymbol{u}^{\beta}]\!](\boldsymbol{x},t)\otimes\boldsymbol{n}^{\boldsymbol{\beta}})^{s} - \Delta\lambda^{p^{m}}\frac{\partial g^{p^{m}}}{\partial\boldsymbol{\sigma}^{\boldsymbol{m}}}\right] + \sum_{f=1}^{nf} k^{f}\left[E^{f}_{rr}\left(\epsilon^{f}_{rr} - \Delta\lambda^{p^{f}}\frac{\partial f^{p^{f}}_{rr}}{\partial {\sigma^{f}}_{rr}}\right)\right.$$
$$\left.\boldsymbol{n}^{\boldsymbol{\beta}}.[\boldsymbol{r}^{f}\otimes\boldsymbol{r}^{f}] + 2G^{f}_{rs}\left(\epsilon^{f}_{rs} - \Delta\lambda^{p^{f}}\frac{\partial f^{p^{f}}_{rs}}{\partial {\sigma^{f}}_{rs}}\right)\boldsymbol{n}^{\boldsymbol{\beta}}.[\boldsymbol{r}^{f}\otimes\boldsymbol{s}^{f}]^{s} + 2G^{f}_{rt}\left(\epsilon^{f}_{rt} - \Delta\lambda^{p^{f}}\frac{\partial f^{p^{f}}_{rt}}{\partial {\sigma^{f}}_{rt}}\right)\boldsymbol{n}^{\boldsymbol{\beta}}.[\boldsymbol{r}^{f}\otimes\boldsymbol{t}^{f}]^{s}\right] \tag{3.2}$$

and after some algebraic operations with bandwidth h we obtain:

$$\mathbb{T}^{c^{\beta}}_{\mathbb{S}} = \boldsymbol{\sigma}^{c^{\beta}}_{\mathbb{S}}.\boldsymbol{n}^{\boldsymbol{\beta}} = \lim_{h\to 0}\frac{1}{hr_{\mathbb{S}}}k^{m}q_{\mathbb{S}}\boldsymbol{n}^{\boldsymbol{\beta}}.\mathbb{C}^{e^{m}} : \left[h\bar{\boldsymbol{\epsilon}} + (\Delta[\![\boldsymbol{u}^{\beta}]\!](\boldsymbol{x},t)\otimes\boldsymbol{n}^{\boldsymbol{\beta}})^{s} - h\underbrace{\Delta\lambda^{p^{m}}\frac{\partial g^{p^{m}}}{\partial\boldsymbol{\sigma}^{\boldsymbol{m}}}}_{\boldsymbol{\epsilon}^{\boldsymbol{p^{m}}}}\right] + \sum_{f=1}^{nf} k^{f}\left[E^{f}_{rr}\left(\epsilon^{f}_{rr} - \Delta\lambda^{p^{f}}\frac{\partial f^{p^{f}}_{rr}}{\partial {\sigma^{f}}_{rr}}\right)\right.$$
$$\left.\boldsymbol{n}^{\boldsymbol{\beta}}.[\boldsymbol{r}^{f}\otimes\boldsymbol{r}^{f}] + 2G^{f}_{rs}\left(\epsilon^{f}_{rs} - \Delta\lambda^{p^{f}}\frac{\partial f^{p^{f}}_{rs}}{\partial {\sigma^{f}}_{rs}}\right)\boldsymbol{n}^{\boldsymbol{\beta}}.[\boldsymbol{r}^{f}\otimes\boldsymbol{s}^{f}]^{s} + 2G^{f}_{rt}\left(\epsilon^{f}_{rt} - \Delta\lambda^{p^{f}}\frac{\partial f^{p^{f}}_{rt}}{\partial {\sigma^{f}}_{rt}}\right)\boldsymbol{n}^{\boldsymbol{\beta}}.[\boldsymbol{r}^{f}\otimes\boldsymbol{t}^{f}]^{s}\right] \tag{3.3}$$

So the point to emphasize is that if the plasticity model of the matrix in compression is characterised by a hardening law, then it is possible to induce a stable response in the material, by neglecting the term that contains h (bandwidth) which affects the plastic deformation as follows:

$$\mathbb{T}_{\mathbb{S}}^{c^{\beta}} = \boldsymbol{\sigma}_{\mathbb{S}}^{c^{\beta}}.\boldsymbol{n}^{\boldsymbol{\beta}} = \lim_{h\to 0}\frac{1}{hr_{\mathbb{S}}}k^{m}q_{\mathbb{S}}\boldsymbol{n}^{\boldsymbol{\beta}}.\mathbb{C}^{e^{m}} : (\Delta[\![\boldsymbol{u}^{\boldsymbol{\beta}}]\!](\boldsymbol{x},t)\otimes\boldsymbol{n}^{\boldsymbol{\beta}})^{s} + \sum_{f=1}^{nf}k^{f}\left[E_{rr}^{f}\left(\epsilon_{rr}^{f} - \Delta\lambda^{p^{f}}\frac{\partial f_{rr}^{p^{f}}}{\partial\sigma^{f}{}_{rr}}\right)\boldsymbol{n}^{\boldsymbol{\beta}}.[\boldsymbol{r}^{f}\otimes\boldsymbol{r}^{f}] + 2G_{rs}^{f}\left(\epsilon_{rs}^{f} - \Delta\lambda^{p^{f}}\frac{\partial f_{rs}^{p^{f}}}{\partial\sigma^{f}{}_{rs}}\right)\boldsymbol{n}^{\boldsymbol{\beta}}.[\boldsymbol{r}^{f}\otimes\boldsymbol{s}^{f}]^{s} + 2G_{rt}^{f}\left(\epsilon_{rt}^{f} - \Delta\lambda^{p^{f}}\frac{\partial f_{rt}^{p^{f}}}{\partial\sigma^{f}{}_{rt}}\right)\boldsymbol{n}^{\boldsymbol{\beta}}.[\boldsymbol{r}^{f}\otimes\boldsymbol{t}^{f}]^{s}\right] \tag{3.4}$$

Then by rearranging the term of normal propagation direction of the fracture multiple surface $\boldsymbol{n}^{\boldsymbol{\beta}}$, it is possible find the acoustic tensor of the matrix $\boldsymbol{Q}^{m^{e}}$ through the following expression:

$$\mathbb{T}_{\mathbb{S}}^{c^{\beta}} = \boldsymbol{\sigma}_{\mathbb{S}}^{c^{\beta}}.\boldsymbol{n}^{\boldsymbol{\beta}} = \lim_{h\to 0}\frac{1}{hr_{\mathbb{S}}}k^{m}q_{\mathbb{S}}\underbrace{(\boldsymbol{n}^{\boldsymbol{\beta}}.\mathbb{C}^{e^{m}}.\boldsymbol{n}^{\boldsymbol{\beta}})}_{\boldsymbol{Q}^{m^{e}}}.\Delta[\![\boldsymbol{u}^{\boldsymbol{\beta}}]\!](\boldsymbol{x},t) + \sum_{f=1}^{nf}k^{f}\left[E_{rr}^{f}\left(\epsilon_{rr}^{f} - \Delta\lambda^{p^{f}}\frac{\partial f_{rr}^{p^{f}}}{\partial\sigma^{f}{}_{rr}}\right)\boldsymbol{n}^{\boldsymbol{\beta}}.[\boldsymbol{r}^{f}\otimes\boldsymbol{r}^{f}] + 2G_{rs}^{f}\left(\epsilon_{rs}^{f} - \Delta\lambda^{p^{f}}\frac{\partial f_{rs}^{p^{f}}}{\partial\sigma^{f}{}_{rs}}\right)\boldsymbol{n}^{\boldsymbol{\beta}}.[\boldsymbol{r}^{f}\otimes\boldsymbol{s}^{f}]^{s} + 2G_{rt}^{f}\left(\epsilon_{rt}^{f} - \Delta\lambda^{p^{f}}\frac{\partial f_{rt}^{p^{f}}}{\partial\sigma^{f}{}_{rt}}\right)\boldsymbol{n}^{\boldsymbol{\beta}}.[\boldsymbol{r}^{f}\otimes\boldsymbol{t}^{f}]^{s}\right] \tag{3.5}$$

Finally, we can obtain the general expression for the traction vector of the reinforced concrete $\mathbb{T}_{\mathbb{S}}^{c^{\beta}}$ in **Eq. (3.6)**

Box 3.1: *General expression for the traction vector of the composite material*

$$\mathbb{T}_{\mathbb{S}}^{c^{\beta}} = \boldsymbol{\sigma}_{\mathbb{S}}^{c^{\beta}}.\boldsymbol{n}^{\boldsymbol{\beta}} = \underbrace{\lim_{h\to 0}\frac{1}{hr_{\mathbb{S}}}k^{m}q_{\mathbb{S}}\boldsymbol{Q}^{m^{e}}.\Delta[\![\boldsymbol{u}^{\boldsymbol{\beta}}]\!](\boldsymbol{x},t)}_{\text{Term 1}} + \underbrace{\boldsymbol{n}^{\boldsymbol{\beta}}.\left[\sum_{f=1}^{nf}k^{f}\left[E_{rr}^{f}\left(\epsilon_{rr}^{f} - \Delta\lambda^{p^{f}}\frac{\partial f_{rr}^{p^{f}}}{\partial\sigma^{f}{}_{rr}}\right)[\boldsymbol{r}^{f}\otimes\boldsymbol{r}^{f}] + \underbrace{2G_{rs}^{f}\left(\epsilon_{rs}^{f} - \Delta\lambda^{p^{f}}\frac{\partial f_{rs}^{p^{f}}}{\partial\sigma^{f}{}_{rs}}\right)[\boldsymbol{r}^{f}\otimes\boldsymbol{s}^{f}]^{s} + 2G_{rt}^{f}\left(\epsilon_{rt}^{f} - \Delta\lambda^{p^{f}}\frac{\partial f_{rt}^{p^{f}}}{\partial\sigma^{f}{}_{rt}}\right)[\boldsymbol{r}^{f}\otimes\boldsymbol{t}^{f}]^{s}}_{cont.\text{Term 2}}\right]\right]}_{\text{Term 2}} \tag{3.6}$$

Proposition 3.1 *Find the discrete internal variable for the behaviour of the matrix using the isotropic damage model, employed in the behaviour of the composite material.*

In order to explain **Eq. (3.6)**, and find the discrete internal variables, we follow the flow of the above ***eq.*** in the same order and very close to that by Oliver [2] , but incorporating the effects of the reinforcing fibers. The matrix elastic acoustic tensor is positive definite William and Sobh [4] , so the first term in **Eq. (3.6)** implies that, in order for that the traction vector $\mathbb{T}_{\mathbb{S}}^{\mathbf{c}}$ to be bounded, the term over brackets $\Delta[\![\boldsymbol{u}]\!](\boldsymbol{x},t)$ must be different than zero, $\Delta[\![\boldsymbol{u}]\!](\boldsymbol{x},t)\neq 0$. Therefore fulfillment of the mathematical consistency of the first term in **Eq. (3.6)** implies that:

$$\lim_{h\to 0} hr_{\mathbb{S}} \neq 0 \quad \text{iff} \quad \Delta[\![\boldsymbol{u}]\!](\boldsymbol{x},t)\neq 0 \tag{3.7}$$

while **Eq. (3.7)** , it is to define the evolution of the *internal variables* $r_{\mathbb{S}}$, $q_{\mathbb{S}}$, in rate form, to be bounded, depending on a bounded discrete internal variable $\bar{\alpha}$, for the behavior of the matrix, as follows:

Lemma 3.1 *Let us consider the evolution of $r_{\mathbb{S}}$ in* ***Eq. (3.8)***

$$\dot{r}_{\mathbb{S}} = \frac{1}{h}\dot{\bar{\alpha}} \quad \forall t > t_{SD} \tag{3.8}$$

in which, $\bar{\alpha} = 0 \quad \forall t \leq t_{SD}$.

Proof 3.1 *In the same manner like the strain composite tensor, the discrete internal variable $r_{\mathbb{S}}$, can be integrated, for a given time $t \geq t_{SD}$:*

$$r_{\mathbb{S}} = \int_0^t \dot{r}_{\mathbb{S}} dt = \underbrace{r_{WD} + \int_{t_{WD}}^{t_{SD}} \frac{1}{h(\tau_{\boldsymbol{\sigma}^m})}\dot{\bar{\alpha}}\, d\tau_{\boldsymbol{\sigma}^m}}_{:=r_{SD}} + \underbrace{\int_{t_{SD}}^{t} \underbrace{\frac{1}{h}}_{h\equiv k}\dot{\bar{\alpha}}\, d\tau_{\boldsymbol{\sigma}^m}}_{:=r_{const}} = r_{SD} + \frac{1}{h(\tau_{\boldsymbol{\sigma}^m})}\underbrace{\int_{t_{SD}}^{t}\dot{\bar{\alpha}}\, d\tau_{\boldsymbol{\sigma}^m}}_{:=\Delta\bar{\alpha}} \tag{3.9}$$

where the internal variable r_{SD} in time of strong discontinuity can be defined by:

$$r_{SD} = r_{WD} + \int_{t_{WD}}^{t_{SD}} \frac{1}{h(\tau_{\boldsymbol{\sigma}^m})}\dot{\bar{\alpha}}\, d\tau_{\boldsymbol{\sigma}^m} \tag{3.10}$$

and the increment of the discrete internal variable $\Delta\bar{\alpha}$ is defined by the following expression:

$$\Delta\bar{\alpha} = \int_{t_{SD}}^{t} \dot{\bar{\alpha}}\, d\tau_{\boldsymbol{\sigma}^m} \tag{3.11}$$

Thus, the key point to take into account is that the mechanism of formation of a strong discontinuity, consists in the evolution of the bandwidth $h(t)$, decreasing until collapse in k, $h \equiv k$, being k a value as small as the precision of the machine will allows. Then, r_{const}, has the following form:

$$r_{const} = \frac{1}{k}\Delta\bar{\alpha} \tag{3.12}$$

Given that h lies in k in the time of strong discontinuity, we can substituting the ***Eqs.(3.10)*** *and* ***(3.11)*** *as in* ***Eq. (3.7)****, in the following way:*

$$\lim_{h\to 0} h r_{SD} = \lim_{k\to 0} k r_{SD} = k r_{WD} + \frac{k}{h(\tau_{\boldsymbol{\sigma}^m})}\Delta\bar{\alpha} \neq 0 \tag{3.13}$$

which is a bounding expression. With this in the mind, we are finally able to prove that that the law of evolution of the internal variable $\dot{r}_{\mathbb{S}}$ ***Eq. (3.8)****, that fulfill the condition* ***Eq. (3.7)*** *and making the first term in* ***Eq. (3.6)*** *(matrix behaviour), is compatible with $\Delta[\![\boldsymbol{u}]\!](\boldsymbol{x}, t) \neq 0$, we again substitute the* ***Eqs. (3.10)*** *to* ***(3.13)*** *back in* ***Eq. (3.7)****:*

$$\lim_{h\to 0} h r_{\mathbb{S}} = h r_{SD} + h r_{connst} = h\frac{1}{h}\Delta\bar{\alpha} = \Delta\bar{\alpha} \neq 0 \tag{3.14}$$

which is also a bound expression.

Corollary 3.1 *In view of* ***Eq. (3.14)****, an important corollary to this result is that:*

$$\lim_{h\to 0} h r_{\mathbb{S}} = \Delta\bar{\alpha} \tag{3.15}$$

□

For the matrix model (discrete damage model) to be complete, it is necessary to incorporate the hardening-softening rule as follows:

$$\dot{q}_{\mathbb{S}} = \frac{\partial q}{\partial r}\dot{r}_{\mathbb{S}} \tag{3.16}$$

However, substituting **Eq. (3.8)** into **Eq. (3.16)** yields

$$\dot{q}_{\mathbb{S}} = \frac{\partial q}{\partial r}\frac{1}{h}\dot{\alpha} \tag{3.17}$$

As demonstrated in **Proof 3.1** , $\dot{r}_{\mathbb{S}}$ is a function of $\dot{\alpha}$ and is bounded. Therefore, we can conclude that $\dot{q}_{\mathbb{S}}$ is also bounded, at the time of strong discontinuity

$$\lim_{h\to 0}\frac{\partial q}{\partial r}\frac{1}{h} = \mathbb{H}^m\frac{1}{h} = \bar{\mathbb{H}}^m \tag{3.18}$$

into which the discrete softening parameter for the matrix $\bar{\mathbb{H}}^m$ is incorporated.

Corollary 3.2 *Another important corollary to this result is that, for the above equation to be fulfilled, it is possible to obtain the continuum softening parameter for the matrix $\mathbb{H}^m$, in terms of the bandwidth h and the discrete softening parameter $\bar{\mathbb{H}}^m$ parameters, by the following expression:*

$$\mathbb{H}^m(t) = h(t)\bar{\mathbb{H}}^m \quad \forall t \geq t_{WD} \tag{3.19}$$

if the expression **Eq. (3.18)** is substituted into **Eq. (3.17)** , we can obtain in a natural manner a discrete softening law

$$\dot{q}_{\mathbb{S}} = \bar{\mathbb{H}}\dot{\alpha} \qquad q_{\mathbb{S}} \in [o, r_0] \qquad \forall t \geq t_{SD} \tag{3.20}$$

Which, in turn can also be integrated as in **Eq. (3.9)**

$$q_{\mathbb{S}} = \bar{q}(\Delta\bar{\alpha}) = q_{SD} + \int_{t_{SD}}^{t} \bar{\mathbb{H}}\dot{\alpha}\, d\tau_{\sigma^m} \tag{3.21}$$

Remark 3.1 *For the tractions vector of composite constitutive model to be complete, it is necessary to analyze the second term in **Eq. (3.6)**, i.e. the behaviour of the fibers. However, the fiber model is equipped with a hardening law, (but with $H^f = 0$), in order to induce a stable material response consistent with the behavior of fibers, preventing the second term in **Eq. (3.6)** , from causing the onset of displacement jumps in the composite model, i.e. the cause of the softening of the composite material is the matrix (plain concrete -damage model). This point having been clarified, the traction vector $\mathbb{T}^c_{\mathbb{S}}$, can be obtained by substituting **Eq. (3.15)** into **Eq. (3.6)**, thus yielding:*

Box 3.2: *Final expression for the traction vector of the composite material*

$$\mathbb{T}_{\mathbb{S}}^{c^\beta} = \boldsymbol{\sigma}_{\mathbb{S}}^{c^\beta}.\boldsymbol{n}^\beta = k^m\left[\frac{q_{\mathbb{S}}}{\Delta\tilde{\alpha}}\boldsymbol{Q}^{m^e}.\Delta[\![\boldsymbol{u}^\beta]\!](\boldsymbol{x},t)\right] + \boldsymbol{n}^\beta.\left[\sum_{f=1}^{nf} k^f\left[E_{rr}^f\left(\epsilon_{rr}^f - \Delta\lambda^{p^f}\frac{\partial f_{rr}^{p^f}}{\partial \sigma^f{}_{rr}}\right)[\boldsymbol{r}^f\otimes\boldsymbol{r}^f] + 2G_{rs}^f\left(\epsilon_{rs}^f - \Delta\lambda^{p^f}\frac{\partial f_{rs}^{p^f}}{\partial \sigma^f{}_{rs}}\right)[\boldsymbol{r}^f\otimes\boldsymbol{s}^f]^s + 2G_{rt}^f\left(\epsilon_{rt}^f - \Delta\lambda^{p^f}\frac{\partial f_{rt}^{p^f}}{\partial \sigma^f{}_{rt}}\right)[\boldsymbol{r}^f\otimes\boldsymbol{t}^f]^s\right]\right] \quad (3.22)$$

3.2 Discrete free energy for the composite material

Let us now consider the discrete free energy for the composite material using a free energy function for a given particle, situated at the discontinuity interface $\mathbb{S}$, considering the composite kinematics described in the previous chapter:

$$\begin{aligned}\psi^c(\epsilon^c, r, \alpha^{p^m}, \theta_{f=1}^{nf}[r_{rr}^f, r_{rs}^f, r_{rt}^f])|_{\boldsymbol{x}\in\mathbb{S}} &= \psi_{\mathbb{S}}^c(\epsilon_{\mathbb{S}}^c, r_{\mathbb{S}}, \alpha^{p^m}, \theta_{f=1}^{nf}[r_{rr}^f, r_{rs}^f, r_{rt}^f]) \\ &= \psi_{\mathbb{S}}^c(\bar{\boldsymbol{\epsilon}}^c + \frac{1}{k}(\sum_{\beta=1}^{N_S}\boldsymbol{\Delta}[\![\boldsymbol{u}^\beta]\!]\otimes\boldsymbol{n}^\beta)^s, r_{\mathbb{S}}, \alpha^{p^m}, \theta_{f=1}^{nf}[r_{rr}^f, r_{rs}^f, r_{rt}^f]) \\ &= \hat{\psi}_{\mathbb{S}}^c(\bar{\boldsymbol{\epsilon}}^c, \Delta[\![\boldsymbol{u}^\beta]\!], r_{\mathbb{S}}, \alpha^{p^m}, \theta_{f=1}^{nf}[r_{rr}^f, r_{rs}^f, r_{rt}^f]) \end{aligned} \quad (3.23)$$

The symbol $\theta_{f=1}^{nf}$ in **Eq. (3.23)** is used only to represent the multiple fibers embedded in composite material. With the above **eq.** in the mind, is straightforward to substitute this expression as:

$$\begin{aligned}\hat{\psi}_{\mathbb{S}}^c &= k^m\psi_{\mathbb{S}}^m + \sum_{f=1}^{nf} k^f\psi^f \\ &= k^m\left[\frac{q_{\mathbb{S}}}{r_{\mathbb{S}}}\psi^0(\underbrace{\bar{\boldsymbol{\epsilon}}^c + \frac{1}{k}(\sum_{\beta=1}^{N_S}\boldsymbol{\Delta}[\![\boldsymbol{u}^\beta]\!]\otimes\boldsymbol{n}^\beta)^s}_{\boldsymbol{\epsilon}_{\mathbb{S}}^c}) + \psi^p(\alpha^m)\right] + \sum_{f=1}^{nf} k^f\left[\underbrace{\frac{1}{2}\epsilon^{e^f}E^f\epsilon^{e^f} + \psi^p(r_{rr}^f)}_{\text{axial effect}}\cdots\right. \\ &\left. + \underbrace{\frac{1}{2}\epsilon^{e^f}E^f\epsilon^{e^f} + \psi^p(r_{rs}^f)}_{\text{shear effect}} + \underbrace{\frac{1}{2}\epsilon^{e^f}E^f\epsilon^{e^f} + \psi^p(r_{rt}^f)}_{\text{shear effect}}\right]\end{aligned} \quad (3.24)$$

For convenience, let us to obtain the derivative of $\boldsymbol{\epsilon}_{\mathbb{S}}^c$ with respect to $\boldsymbol{\Delta}[\![\boldsymbol{u}]\!]$ as follows:

$$\begin{aligned}\frac{\partial\boldsymbol{\epsilon}_{\mathbb{S}}^c}{\partial\boldsymbol{\Delta}[\![\boldsymbol{u}^\beta]\!]} &= \frac{\partial\left[\frac{1}{2h}\boldsymbol{\Delta}[\![\boldsymbol{u}^\beta]\!]\otimes\boldsymbol{n}^\beta + \boldsymbol{n}^\beta\otimes\boldsymbol{\Delta}[\![\boldsymbol{u}^\beta]\!]\right]}{\partial\boldsymbol{\Delta}[\![\boldsymbol{u}^\beta]\!]} \\ &= \frac{1}{2h}(\mathbf{1}\otimes\boldsymbol{n}^\beta + \boldsymbol{n}^\beta\otimes\mathbf{1}) = \frac{1}{h}(\mathbf{1}\otimes\boldsymbol{n}^\beta)^s\end{aligned} \quad (3.25)$$

Now, it is really simple to obtain the derivative of $\hat{\psi}_{\mathbb{S}}^c$ with respect to $\boldsymbol{\Delta}[\![\boldsymbol{u}]\!]$ by incorporating the composite stress tensor and **Eq. (3.25)**:

$$\frac{\partial \hat{\psi}^c_{\mathbb{S}}}{\partial \boldsymbol{\Delta}[\![\boldsymbol{u}^{\beta}]\!]} = \underbrace{\frac{\partial \hat{\psi}^c_{\mathbb{S}}}{\partial \boldsymbol{\epsilon}^c_{\mathbb{S}}}}_{\boldsymbol{\sigma}^{c^{\beta}}_{\mathbb{S}}} : \frac{\partial \boldsymbol{\epsilon}^c_{\mathbb{S}}}{\partial \boldsymbol{\Delta}[\![\boldsymbol{u}^{\beta}]\!]} = \frac{1}{h}\boldsymbol{\sigma}^{c^{\beta}}_{\mathbb{S}} . \boldsymbol{n}^{\beta} = \frac{1}{h}\mathbb{T}^{c^{\beta}}_{\mathbb{S}} \tag{3.26}$$

Given that h lies in k in the time of strong discontinuity, of **Eq. (3.26)**, it is simple to obtain that:

$$\mathbb{T}^{c^{\beta}}_{\mathbb{S}} = \frac{\partial [\lim_{h\to 0} h\hat{\psi}^c_{\mathbb{S}}]}{\partial \boldsymbol{\Delta}[\![\boldsymbol{u}^{\beta}]\!]} = \frac{\partial [\varphi^c_{\mathbb{S}}]}{\partial \boldsymbol{\Delta}[\![\boldsymbol{u}^{\beta}]\!]} \tag{3.27}$$

in which the composite discrete free energy $\varphi^c_{\mathbb{S}} = \lim_{h\to 0} h\hat{\psi}^c_{\mathbb{S}}$ has been considered.

3.3 Composite strong discontinuity conditions

As shown in *Section(3.1)* and *Section(3.2)* , the discrete composite traction vector $\mathbb{T}^c_{\mathbb{S}}$, as well as, the discrete composite free energy $\varphi^c_{\mathbb{S}}$ according to that proposed by Simo et al. [3] , where the only significant difference is the incorporation of the mechanical behavior of reinforced concrete. However, in order to find the so-called composite strong discontinuity equation, as in Oliver [1] , it is necessary to obtain an expression, in terms of $\sigma^c_{\mathbb{S}}$ and $\Delta[\![\boldsymbol{u}]\!]$, to fulfill such a condition in terms of $\boldsymbol{\epsilon}^c_{\mathbb{S}}$. Neglecting the term of the matrix plastic deformation $\boldsymbol{\epsilon}^{P^m} = \Delta\lambda^{P^m}\frac{\partial g^{P^m}}{\partial \boldsymbol{\sigma}^m}$ in compression, by performing some algebraic operations with the bandwidth h, for $t > t_{SD}$ we are able to obtain:

$$\begin{aligned}\boldsymbol{\sigma}^{c^{\beta}}_{\mathbb{S}} =& \lim_{h\to 0}\frac{1}{hr_{\mathbb{S}}}k^m q_{\mathbb{S}}\boldsymbol{C}^{m^e} : (\Delta[\![\boldsymbol{u}^{\beta}]\!](\boldsymbol{x},t)\otimes\boldsymbol{n}^{\beta})^s + \sum_{f=1}^{nf} k^f\left[E^f_{rr}\left(\epsilon^f_{rr} - \Delta\lambda^{P^f}\frac{\partial f^{P^f}_{rr}}{\partial \sigma^f{}_{rr}}\right)[\boldsymbol{r}^f\otimes\boldsymbol{r}^f] + \right.\\ & \left. 2G^f_{rs}\left(\epsilon^f_{rs} - \Delta\lambda^{P^f}\frac{\partial f^{P^f}_{rs}}{\partial \sigma^f{}_{rs}}\right)[\boldsymbol{r}^f\otimes\boldsymbol{s}^f]^s + 2G^f_{rt}\left(\epsilon^f_{rt} - \Delta\lambda^{P^f}\frac{\partial f^{P^f}_{rt}}{\partial \sigma^f{}_{rt}}\right)[\boldsymbol{r}^f\otimes\boldsymbol{t}^f]^s\right]\end{aligned} \tag{3.28}$$

Now, we can use the **Corollary 3.1** (**Eq. (3.15)**) in **Eq. (3.28)** as follows:

Box 3.3: *General expression for the composite material discrete stress tensor*

$$\begin{aligned}\boldsymbol{\sigma}^{c^{\beta}}_{\mathbb{S}} =& k^m\frac{q_{\mathbb{S}}}{\Delta\bar{\alpha}}\boldsymbol{C}^{m^e} : (\Delta[\![\boldsymbol{u}^{\beta}]\!](\boldsymbol{x},t)\otimes\boldsymbol{n}^{\beta})^s + \sum_{f=1}^{nf} k^f\left[E^f_{rr}\left(\epsilon^f_{rr} - \Delta\lambda^{P^f}\frac{\partial f^{P^f}_{rr}}{\partial \sigma^f{}_{rr}}\right)[\boldsymbol{r}^f\otimes\boldsymbol{r}^f] + \right.\\ & \left. 2G^f_{rs}\left(\epsilon^f_{rs} - \Delta\lambda^{P^f}\frac{\partial f^{P^f}_{rs}}{\partial \sigma^f{}_{rs}}\right)[\boldsymbol{r}^f\otimes\boldsymbol{s}^f]^s + 2G^f_{rt}\left(\epsilon^f_{rt} - \Delta\lambda^{P^f}\frac{\partial f^{P^f}_{rt}}{\partial \sigma^f{}_{rt}}\right)[\boldsymbol{r}^f\otimes\boldsymbol{t}^f]^s\right]\end{aligned} \tag{3.29}$$

Finally, by means of some algebraic operations it is possible to obtain a general expression which provides a relationship between $(\Delta[\![\boldsymbol{u}]\!](\boldsymbol{x},t)$ and $\boldsymbol{\sigma}^c_{\mathbb{S}}$, which must be fulfilled for all $t \geq t_{SD}$:

Box 3.4: *General expression for the composite material multiple surface equation*

$$(\Delta[\![\boldsymbol{u}^{\beta}]\!](\boldsymbol{x},t)\otimes\boldsymbol{n})^{s}=k^{m^{-1}}\frac{\Delta\bar{\alpha}}{q_{\mathbb{S}}}\boldsymbol{C}^{\boldsymbol{m}^{\boldsymbol{e}-\mathbf{1}}}:\left[\boldsymbol{\sigma}_{\mathbb{S}}^{c^{\beta}}-\sum_{f=1}^{nf}k^{f}\left[E_{rr}^{f}\left(\epsilon_{rr}^{f}-\Delta\lambda^{p^{f}}\frac{\partial f_{rr}^{p^{f}}}{\partial\sigma^{f}{}_{rr}}\right)[\boldsymbol{r}^{f}\otimes\boldsymbol{r}^{f}]+\right.\right.$$
$$\left.\left.2G_{rs}^{f}\left(\epsilon_{rs}^{f}-\Delta\lambda^{p^{f}}\frac{\partial f_{rs}^{p^{f}}}{\partial\sigma^{f}{}_{rs}}\right)[\boldsymbol{r}^{f}\otimes\boldsymbol{s}^{f}]^{s}+2G_{rt}^{f}\left(\epsilon_{rt}^{f}-\Delta\lambda^{p^{f}}\frac{\partial f_{rt}^{p^{f}}}{\partial\sigma^{f}{}_{rt}}\right)[\boldsymbol{r}^{f}\otimes\boldsymbol{t}^{f}]^{s}\right]\right] \tag{3.30}$$

References

[1] Oliver, J. (1996). Modelling strong discontinuities in solid mechanics via strain softening constitutive equations. part 1: Fundamentals. *International journal for numerical methods in engineering*, 39:3575–3600. 30

[2] Oliver, J. (2000). On the discrete constitutive models induced by strong discontinuity kinematics and continuum constitutive equations. *International journal of solids and structures*, 37:7207–7229. 26

[3] Simo, J., Oliver, J., and Armero, F. (1993). An analysis of strong discontinuities induced by strain-softening in rate-independent inelastic solids. *Computational mechanics*, 12(5):277–296. 30

[4] William, K. and Sobh, N. (1987). *Bifurcation analysis of tangential material operator*, volume 2 of *Transient-Dynamic analysis and constitutive laws foe engineering materials.* In:Pande, G.N.Middleton. J.(Eds.). 26

Part IV

Conclusions and lines of development

4

Conclusions, final remarks and outline for future work

In the context of rate independent solids a framework has been established to study of the phenomena of multiple localization surfaces of failure. To this end, we present the strain localization problems in three-dimensional RC members. A necessary condition for that this phenomenon occurs is the loss of ellipticity of the composite acoustic tensor. However, when we add the reinforcement fibers, these fibers have a effect of close the cracks and not allow the crack evolves, therefore it is important to mention that, each fiber evolve mechanically until plasticize, once plasticize, the softening is not allowed. Allowing the matrix is responsible for obtaining the material failure process. Another mechanical problem when trying to model numerically(RC) members, is the introduction of steel stirrups. These steel stirrups generate a core the high strength inside of the structural member. For this reason, we using in this part the composite constitutive model design during my Ph.d, where this core is modeled by an elasto-plastic-damage behavior, and we incorporate multiple fibers in different directions (modeled by elasto-plastic behavior of each fiber that make up this material point).At this point it is worth noting that, the mechanical behavior of each compound of the composite material, is modeled separately, and the global response is obtained by an assembly of all contributions, by means the use of the rule of mixture theory. For this reason, is important introduce in an adequate manner the field of the displacement. In another words, if we consider the phenomena of multiple surface of failure, the composite discrete traction vector change, and is a compulsory condition, in order to establish a general framework, so, several directions of future works suggest themselves:

- This work has been carried out for rate independent, isothermal solids. One natural extension would be to include rate and thermal effects and solve the coupled thermo-mechanical problem.
- Also this work was carried only in the small deformation regime, for that reason it would be interesting to address the issue of large deformations, in search of a bifurcation time most precise.
- A new tracking algorithm for the cracks applied to the composite material, and the dynamic problem, and see what happens with the phenomenon of branching in members of reinforced concrete.
- For that the structural curve is more adjusted, the mechanical behavior of aggregate can be consider.

- **However, the most important point to comment is: it is possible generate a new framework, in the line of two-scale homogenization scheme: The FE^2. To this end, could be interesting see how is the form of the composite discrete traction vector in a micro-scale manner.**

References

Author Index

Subjects